

## The Circular Dipole

Karthik Lakshmanan<sup>1</sup>, Martijn Cloos<sup>1</sup>, Ricardo Lattanzi<sup>1</sup>, Daniel Sodickson<sup>1</sup>, Dmitry Novikov<sup>1</sup>, and Graham Wiggins<sup>1</sup>  
<sup>1</sup>Department of Radiology, New York University School of Medicine, New York, New York, United States

At fields of 7 Tesla and higher, increasing interest has been shown in the application of electric dipole antennas as transmit and receive coils for MR imaging<sup>1-3</sup>. There are challenges in applying electric dipole antenna designs for MR imaging. A self-resonant half wavelength dipole antenna is between 35 and 50 cm long, depending on its proximity to tissue, inconveniently long for many applications. Placing a slab of high dielectric material between the dipole and the body shortens the length, but such blocks of material are bulky, and high SAR may be generated at the edges of the block<sup>4</sup>. Inclusion of lumped element inductors or meanders along the length of the dipole antenna can shorten it, but often at the cost of increased losses. Typical measures used to decouple arrays of surface coil loops such as overlap or decoupling circuitry are not obviously applicable to dipole antennas, limiting the density of dipole antenna placement with current designs. To achieve best performance at 7T a combination of magnetic loop and electric dipole elements is desired<sup>5,6</sup>, doubling the number of elements needed to provide sample coverage and diverse antenna properties.

We investigate here the circular dipole, consisting of a circular conductor with a feed point on one side and a gap on the other Fig. 1, inspired by the halo antenna. This design is found to have benefits compared to a straight half-wavelength self-resonant dipole antenna in terms of  $B_1^+$  efficiency, compactness, decoupling of neighboring elements and the potential for capturing magnetic and electric dipole fields in a single element.

**Methods:** Full wave electromagnetic simulations were performed with the FDTD method (CST Microwave Studio). The coil was modeled as a flat conductor strip 5 cm wide forming a circle with inner diameter of 16 cm (Fig 1). A drive port is placed at a 5 mm gap in the conductor, and with a 2 cm gap in the far side of the circle the antenna was resonant at 297.2 MHz. This was placed 2 cm above a 40 x 25 x 80 cm rectangular block of material with  $\epsilon_r=59$ ,  $\sigma=0.77$ . S11 match of -20dB was achieved by placing a 6.8 pF capacitor in parallel with the drive port. A straight dipole antenna was also simulated 40 cm long with conductor width of 5 cm on the same phantom. A match of -16 dB was achieved by placing a 3.9 pF capacitor in parallel with the drive port. The simulated SNR was calculated by using the Kellman method<sup>7</sup>.

**Results:** Simulated  $B_1^+$  maps for the circular and straight dipole antennas are shown in Figure 2. The circular dipole creates greater excitation near the coil, while still having lower  $B_1^+$  at depth compared to the straight dipole. The peak 10g averaged SAR was higher for the circular dipole (.7247 compared to .4874 for the straight dipole), but when  $B_1^+$  is normalized by dividing by the square root of peak SAR the resulting  $B_1^+$  maps still show better performance near the circular dipole (Figure 3). This sagittal slice also shows the reduced z-extent of the excitation created by the circular dipole compared to the straight dipole.

Examination of the B-vector evolution with time in the simulation (not shown) reveals that there are regions near the circular dipole where circular polarization is produced, whereas the excitation is almost completely linear immediately below the straight dipole. This behavior is summarized in Figures 4 & 5 which show the degree of correct circular polarization by plotting  $(|B_1^+| / |B_1|)^2$ . A value of 2 represents  $B_1$  which is completely circularly polarized in the correct sense, 1 = linear polarization and 0 = anti-quadrature polarization. A substantial amount of circular polarization is produced by the circular dipole compared to almost none for the straight dipole. This is presumably due to the loop-like structure of the circular dipole and the eddy currents induced in the sample<sup>8</sup>. The  $B_1^+$  profile of the circular and straight dipole along the phantom depth is shown in figure 6. The profile shows that circular dipoles produce higher  $B_1^+$  at depths between 5 and 10 cm. Between 10 and 15 cm the circular dipole and the straight dipole produce similar  $B_1^+$ . The straight dipole is better beyond 15 cm.

Simulated SNR maps are shown in figure 7. At shallow depths 5-10 cm the circular dipoles show better SNR performance. We attribute this to circular dipoles being sensitive to both magnetic and electric dipole fields. Between 10 and 15 cm the SNR performance is almost similar and the straight dipole starts to win out after 15 cm

**Discussion:** The circular polarization created by the circular dipole suggests that it should be sensitive both to electric and magnetic dipole fields, potentially offering better performance than either a traditional loop or straight dipole alone. This is supported by considering the current distribution on the circular dipole Figure 8. This may be considered as a linear superposition of a uniform loop of current and a pattern with current traveling in opposite directions around the loop on opposite sides. This latter current pattern has a net electric dipole moment, indicated by the dotted arrow. This has been demonstrated analytically for loop antennas with non-uniform current<sup>9</sup>. So far we do not have data to demonstrate enhanced performance due to the sensitivity to magnetic and electric dipole fields, but studies are currently underway. It has proven possible to place circular dipoles in close proximity to each other (spaced every 14 cm for these 16cm diameter elements) in an arrangement similar to overlapped loop coils. This opens up the possibility of tiling a surface with a large number of circular dipoles to reap the advantages of highly parallel coil arrays.

### References:

- [1] Raaijmakers AJE. ISMRM 2013 p4382 [2] Wiggins G. ISMRM 2012:541. [3] Graessl A. ISMRM 2013:0395 [4] Raaijmakers AJE. Magn Reson Med 2011 66(5):1488-97. [5] Lattanzi R. MRM 68:286-304 (2012) [6] Wiggins G. ISMRM 2013 p2737 [7] Kellman P. Magn Reson Med 2005 54(6):1439-47 [8] Zhang B. ISMRM 2012:2816. [9] Horner F. Properties of Loop Aerials, The Wireless Engineer, Vol. 25, Aug. 1948 p254-259

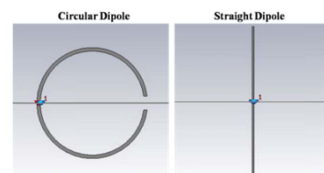


Figure 1. Circular & Straight Dipole Schematic

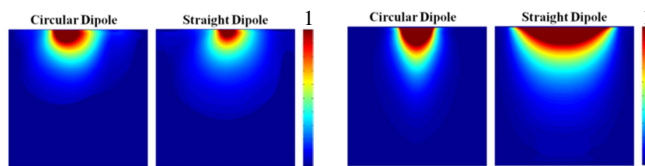


Figure 2. Simulated  $B_1^+$  Central Axial Slice

Figure 3. Simulated  $B_1^+$  in a sagittal slice, normalized for peak 10g SAR

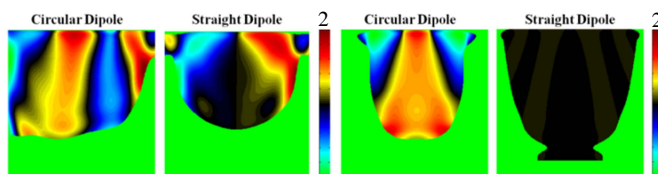


Figure 4. Degree of Circular polarization of  $B_1$ - Axial

Figure 5. Degree of Circular polarization of  $B_1$ - Sagittal

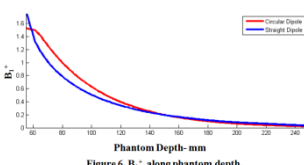


Figure 6.  $B_1^+$  along phantom depth.

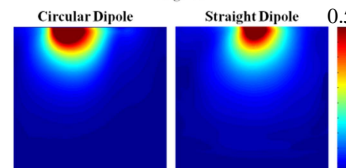


Figure 7. Simulated SNR Central Axial Slice

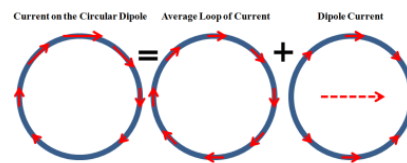


Figure 8. Schematic of current distribution on a circular dipole - A linear superposition of a uniform loop of current, with an electric dipole current moment.